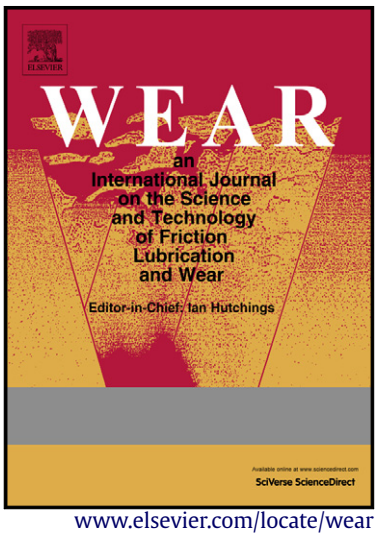

www.elsevier.com/locate/wear

Frictional behavior of self-adaptive nanostructural Mo–Se–C coatings in different sliding conditions

F. Gustavsson, S. Jacobson, A. Cavaleiro, T. Polcar

PII: S0043-1648(13)00221-4
DOI: http://dx.doi.org/10.1016/j.wear.2013.03.032
Reference: WEA100682

To appear in: *Wear*

Received date: 23 January 2013
Revised date: 9 March 2013
Accepted date: 18 March 2013

Cite this article as: F. Gustavsson, S. Jacobson, A. Cavaleiro, T. Polcar, Frictional behavior of self-adaptive nanostructural Mo–Se–C coatings in different sliding conditions, *Wear,* http://dx.doi.org/10.1016/j.wear.2013.03.032

Frictional behavior of self-adaptive nanostructural Mo-Se-C coatings in different sliding conditions

F. Gustavsson[a], S. Jacobson[a], A. Cavaleiro[b] and T. Polcar[c*]

a) The Ångström Tribomaterials Group, Applied Materials Science, Department of Engineering Sciences, Uppsala University, Box 534, 751 21 Uppsala, Sweden

b) SEG-CEMUC - Department of Mechanical Engineering, University of Coimbra, Rua Luís Reis Santos, P-3030 788 Coimbra, Portugal

c) Department of Control Engineering, Faculty of Electrical Engineering, Czech Technical University in Prague, Technická 2, Prague 6, Czech Republic

* Corresponding author – e-mail polcar@fel.cvut.cz; Tel. +420 22435 7598

Abstract

Sliding properties of Mo-Se-C coatings with two different carbon content deposited by magnetron sputtering were investigated in different sliding environments (argon, nitrogen, dry and humid air). Both coatings had a structure that was identified as randomly oriented structures of $MoSe_2$ embedded into amorphous carbon matrix. The worn surfaces, i.e. the wear tracks and the wear scars of the balls, were analyzed by optical microscopy, Raman spectroscopy and scanning electron microscopy. The material transferred to the ball steel surfaces was almost exclusively $MoSe_2$, whereas the wear tracks on the coatings were more complex, with areas rich in $MoSe_2$ and areas similar to that of as-deposited coatings.

The friction was lowest in argon (0.012 at a load of 10 N) and highest in humid air, but still remarkably low; as best 0.05 at 10 N load; however, the exceptionally low wear rate was almost identical. Thus, we focused our detailed analysis on these two examples to understand the mechanisms responsible for the difference between the friction coefficients. SEM, EDX, XPS, Raman and TEM with EELS and EDX were applied to investigate the composition and structure of localized spots of interest on the tested surfaces. In both cases, we observed well-ordered $MoSe_2$ tribofilms with negligible amount of oxides. Carbon was not present in the sliding interfaces, although large amount of carbon was found outside the contacts on both surfaces. Based on our investigations, we suggest the increase in friction of Mo-Se-C in humid air is primarily due to the increase in shear strength of the $MoSe_2$ structure by the presence of water molecules in the sliding interface.

Keywords: **solid lubricants; MoSe2; friction; tribolayer; self-adaptive structure**

1 Introduction

Solid lubricant coatings based on transition metal dichalcogenides (TMDs) constitute a group of promising candidates for applications where liquid lubrication is not wanted or possible. The excellent frictional properties of the layered form of TMDs are attributed to the weak interactions between adjacent molecular layers, resulting in very low shear strengths. Unfortunately, the ultra-low friction is limited to sliding in vacuum due to rapid oxidation and, particularly, detrimental effect of water vapor on friction [1]. TMDs are often used as thin films, and magnetron sputtering is the most versatile and used deposition process. The major drawbacks of pure TMD coatings are low adhesion to the substrate, porous structure

and low hardness. When TMDs are sliding in humid air, they exhibit relatively high friction (~0.2) combined with high wear. To reduce the sensitivity to humidity and to improve the mechanical properties, TMDs have been doped or alloyed with other elements. Significant improvements in the hardness, adhesion to the substrate or wear resistance have been reported [2,3,4]. However, the reduction of friction in humid air is still a challenge [5,6,7].

The majority of studies dealing with TMDs have been aimed at disulfides (MoS_2 and WS_2). An alternative route towards low friction in humid air is the development of coatings based on Se, e.g. $MoSe_2$ and WSe_2. These diselenides have shown higher temperature stability and lower sensitivity to humidity than the corresponding sulfur based materials [8,9,10,11], although the underlying reason is still not clear. Considering oxidation, Johnson described $MoSe_2$ as having lower activation energy than both MoS_2 and WS_2, but that the oxidation of MoS_2 was much more temperature sensitive than $MoSe_2$ [8]. MoS_2 started to oxidize at lower temperatures than $MoSe_2$ and WS_2, but at temperatures of ~450^{o}C, however, diselenides and disulfides exhibited the same oxidation rate. In this study, the diselenides were substoichiometric in selenium while the disulfide coatings were much closer to ideal stoichiometry [11]. The effect of air humidity on oxidation of diselenides at room temperature is not known.

Carbon has been the dominant, and the most successful, alloy element to achieve both good mechanical and tribological properties in humid air [12,13]. In a previous study, we demonstrated that Mo-Se-C coatings can provide very low friction in humid air due to easy arrangement of the coating nanostructure to the sliding process [14]. There are also results showing that carbon has a synergistic effect on the friction performance of MoS_2 in humid air, with the main suggestion that it works as a diffusion barrier for further oxidation [15].

Here we present the tribological properties of molybdenum diselenide coatings, co-sputtered with carbon, in unlubricated sliding contact against steel in four atmospheres (Ar, N_2, dry air,

and humid air). Our aim is to shed light on the role of atmosphere on the sliding of Mo-Se-C, particularly the effect of air humidity on the friction and wear. Thus, special attention has been paid to the analysis of the worn surfaces.

2. Experimental Details

The two coatings tested were deposited by r.f. magnetron sputtering in argon atmosphere from a graphite target with pellets of pure $MoSe_2$ uniformly distributed in the erosion zone, as shown in detail in our previous study [16]. A two-planar-cathode Edwards E306 machine with a 20 dm^3 chamber was used for the deposition process. Prior to deposition the chamber was pumped down to 10^{-4} Pa. The working argon pressure was 0.75 Pa and the target power density was 8 Wcm^{-2}. The coatings were deposited on M2 (AISI) steel substrates with a hardness of ~9 GPa and on Si wafers; the target-to-substrate distance was approx. 10 cm. An approximately 300 nm thick titanium interlayer was first deposited to improve the adhesion of the coatings. Different carbon contents in the coatings were achieved by varying the number of $MoSe_2$ pellets. The coating thickness was evaluated by cross-sectioned coated Si wafers observed in a scanning electron microscope (SEM). X-ray diffraction (XRD) in glancing mode (Co Kα radiation) and transmission electron microscopy (TEM) were used to characterize the microstructure of the coatings. Chemical bonding was investigated using X-ray photoelectron spectroscopy (XPS). The chemical composition was measured with electron probe microanalysis (EPMA). The coating hardness was measured using depth-sensing nanoindentation with the method developed by Oliver and Pharr [17]. Tribological tests were performed in a ball-on-disc tribometer, using 6 mm diameter 100Cr6 steel balls with a hardness of ~7 GPa as counterparts. The setup included a closed hood allowing control of the atmosphere. The tests were performed in Ar, N_2, dry air (relative humidity < 1%) and humid air (relative humidity 55-60%). When testing in Ar, N_2 or dry air, the chamber was filled with

the gas about 30 minutes before the start of the test, and then continually flooded during the whole test. To avoid the inflow of air, the working chamber was slightly over-pressurized. The tests were performed under three loads (2, 5 and 10 N) in all four atmospheres; the maximum Hertzian initial contact pressure was 0.48, 0.65 and 0.83 GPa, respectively. The test duration was 10 000 cycles corresponding to a sliding distance of 157 m. The sliding speed was 0.1 m s^{-1}. Each tribological test was repeated twice; average values of friction and wear rates are presented in the paper.

All worn surfaces were investigated using light optical microscopy (LOM) and SEM equipped with Energy Dispersive X-Ray spectroscopy (EDX). The wear volumes were calculated from the cross section areas measured using white light interferometry in a WYKO NT1100 optical profilometer. Specific wear rates were calculated as worn volume per sliding distance and load.

Based on the tribological results, the wear tracks formed on the MoSe-61C coating, and the corresponding counter surfaces, tested in Ar and humid air were selected for deeper analysis of the frictional mechanisms and, particularly, the influence of humidity. These worn surfaces were investigated using an SEM (Zeiss Leo 1550) equipped for energy dispersive X-ray spectroscopy (EDX) with an Oxford Silicon Drift Detector. XPS in a PHI Quantum 2000 with monochromatic Al Kα radiation was used to gain information about chemical bonds in the transfer films formed on the counter surfaces. All samples were mildly cleaned by sputter etching for 5 min with Ar^+ ions before the first acquisition, then sputtered another 5 min followed by a second acquisition. Before a third acquisition, the sample was sputter etched for another 15 min, leading to a total sputtering time of 25 min. This was done to ensure that the thin layer of surface contamination due to the exposal to air after tests had been penetrated in at least one of the points. A low acceleration voltage (200 V) was selected to minimize the effect of preferential sputtering [18,19]. The spot size for acquisition was 200 μm^2. Gausian-

Lorentzian function was used to fit XPS peaks. Further, Raman spectroscopy was performed in a Renishaw micro-Raman system with 514 nm wavelength. A 5 μm diameter spot and 2 mW laser power was used for all acquisitions. The total scan time for each spectrum was 60 s. TEM cross sections were prepared from selected areas using in-situ lift out in a FEI Strata D235 Focused Ion Beam (FIB) instrument, using 30 kV Ga ions. A protective layer of Pt mixed with C was first deposited with the electron beam to protect the surface from becoming damaged by the ion beam. To further minimize the beam damage, only 5 kV ion beam energy was used in the final steps of the sample preparation. For TEM imaging and acquisition of energy filtered elemental maps (EFTEM) a FEI Tecnai F30 ST equipped with a Gatan post column energy filter was used at 300 kV acceleration voltage. Scanning TEM imaging (STEM), STEM EDX and STEM Electron Energy Loss Spectroscopy Spectrum Imaging (EELS-SI), was then performed in a FEI Titan 80-300 Cubed equipped with a probe corrector and a Gatan HR post column spectrometer. For STEM-EELS-SI a monochromator was used and the microscope was run at 200 kV with a camera length of 19 mm. For STEM EDX, 300 kV was used.

3 Results

3.1 Chemical composition and structure

Chemical composition of the two deposited coatings, total thickness (i.e. including Ti interlayer) and hardness are shown in Table 1. The oxygen content was approx. 2 and 3 at.% for MoSe-61C and MoSe-47C, respectively. The oxygen originated from residual atmosphere in the deposition chamber and, particularly, from the porous $MoSe_2$ pellets; a higher number of pellets thus led to a higher oxygen content. It should be pointed out that the chemical composition given in Table 1 excludes oxygen, i.e. sum of Se, Mo, and C is 100%.

Table 1: Composition and properties of the two investigated coatings

Acronym	Carbon content (at%)	Se/Mo ratio	Thickness (μm)	Hardness (GPa)
MoSe-61C	61	1.72	2.0±0.1	3.2±0.2
MoSe-47C	47	1.66	2.8±0.1	2.1±0.2

The structure and chemical bonding of these coatings were described in detail in our previous works [14,16]. Therefore, we will only briefly summarize the main finding here. Coating cross-sections observed using SEM and TEM showed a dense structure without larger defects or voids. Both coatings, in TEM, exhibited a structure with randomly oriented platelets (length 3-10 nm) of $MoSe_2$ embedded into a carbon matrix, without long range ordering [14]. XPS analysis indicated only Mo-Se, Mo-O and C-C bonds and there was no evidence of molybdenum carbides in the coating. Raman spectroscopy supported the XPS and TEM results by showing carbon peaks and disordered $MoSe_2$ [16]. We should stress here that the chemical coating composition and structure of the coatings were analyzed within three months after the deposition. The coatings were then stored in normal conditions (room temperature, humid air) for 5 years before the tribological test took place. We re-measured the chemical composition and carried out TEM analysis and Raman spectroscopy as well. There were no differences between the results obtained now and 5 years ago. The coatings are thus very stable and could be stored in humid air for long time.

3.2 Sliding tests: friction and wear

Figure 1 summarizes the friction coefficient and wear rate for the MoSe-61C coating; the friction coefficient is calculated as an average value from the entire test. The running-in was very short, the friction stabilized within the first 100 laps and the friction curves were smooth.

In general, the friction coefficient decreases with increasing load, a behavior often seen for this class of solid lubricants. The lowest friction coefficient (0.012) was measured in argon atmosphere at the highest load. However, the friction was very low even in humid air (0.05) for the same load. The significant difference between friction in dry and humid air indicates a detrimental influence of the humidity, whereas the effect of oxygen (compare friction in dry air and nitrogen) was minimal. The difference in friction when sliding in N_2 and Ar atmospheres is noteworthy, since both gases are generally considered inert for this type of tests.

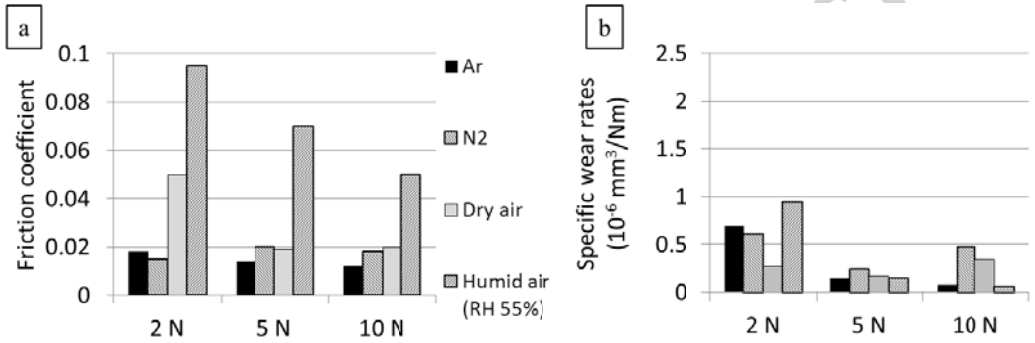

Figure 1: *Tribological results of the MoSe-61C coating sliding against steel balls at three loads in the four atmospheres. (a) Coefficient of friction at steady state. (b) Specific wear rate.*

The wear rate of the MoSe-61C coating was very low in all tested atmospheres. Surprisingly, the wear rate in humid air and argon significantly decreased with increasing load, whereas no such dependence was observed in nitrogen and dry air. The lowest wear rate was achieved in humid air at the highest load. Even considering absolute wear volumes rather than the load specific wear rates, the least worn volume was observed in humid air at the highest load. It is clear that the friction and the wear rates are not directly related.

The MoSe-47C coating showed a somewhat different behavior without a clear load dependence of the friction, see Fig. 2. The higher friction and wear rate resulting when testing in humid air at the highest load were related to partial failure of the coating in the center of the wear track. With this exception, the wear rate was generally similar to that of the MoSe-61C coating. It is well known that this class of material often show a tendency for formation of a transfer film on the counter surface, which has also been thoroughly investigated [20,21]. The transfer film is formed by the combination of direct adhesion of coating material on the ball surface during the contact and partial sintering of wear particles, which are collected and piled up in front of the ball. The contact area on all balls tested here was covered by a relatively thick well-adhering transfer film.

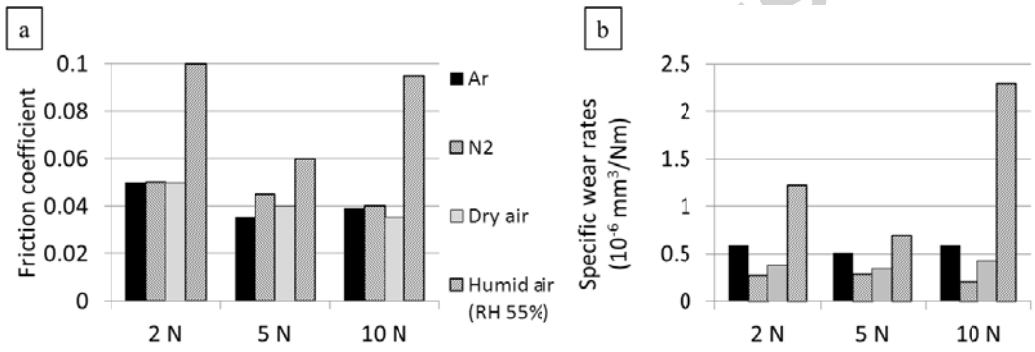

Figure 2: *Tribological results of the MoSe-47C coating sliding against steel balls at three loads in the four atmospheres. (a) Coefficient of friction at steady state. (b) Specific wear rate.*

3.3 Investigation of the worn surfaces – MoSe-47C coating

Figure 3 shows optical images of the wear tracks produced in different atmospheres at the highest load. In dry air, at all loads and for both coatings, the wear tracks showed a striped or patchy appearance in the optical images. Similar patterns also appeared in humid air and nitrogen, but then only in smaller areas. As referred to above, the MoSe-47C coating was worn through at the highest load in the center of the wear track when run in humid air, which

led to higher friction. Also after the high load tests in dry air and nitrogen, microscopic areas of detached coating were observed. However, it seems that in the rest of the tests the coatings supported the load well. Delamination was not observed after the 2 and 5 N load tests, except in small areas in the center of the wear track in humid air in the 2 N load test.

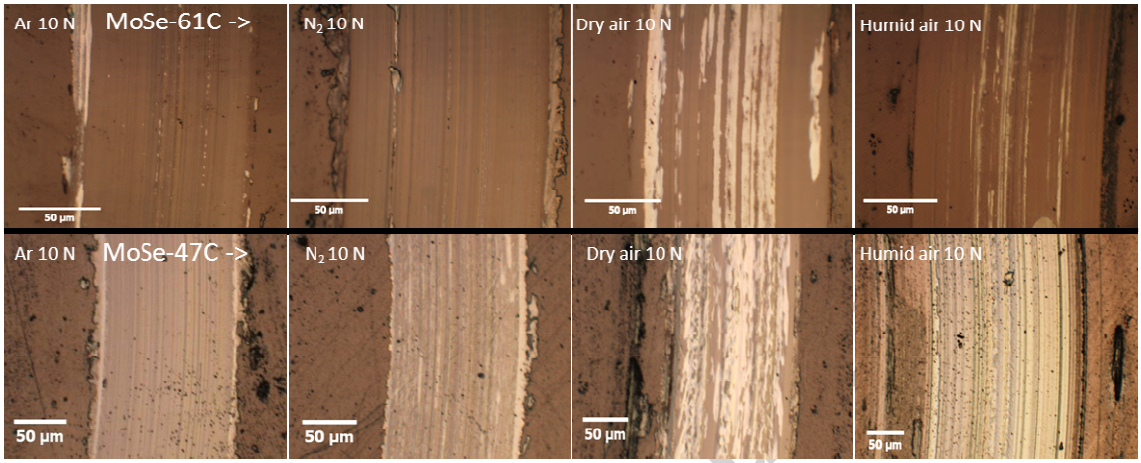

Figure 3: *Optical microscope images of sections of the wear tracks formed in the four environments at 10 N load. Upper row: MoSe-61C, lower row: MoSe-47C. Note the slightly varying magnifications.*

The different contrasts in the wear track observed by optical microscopy, particularly in the case of sliding in dry air, were further investigated. Figure 4 shows a SEM micrograph of the wear track in the coating and the corresponding wear scar on the ball. Backscattered images of the wear track clearly showed that the stripes observed by optical microscopy correspond to different chemical compositions.

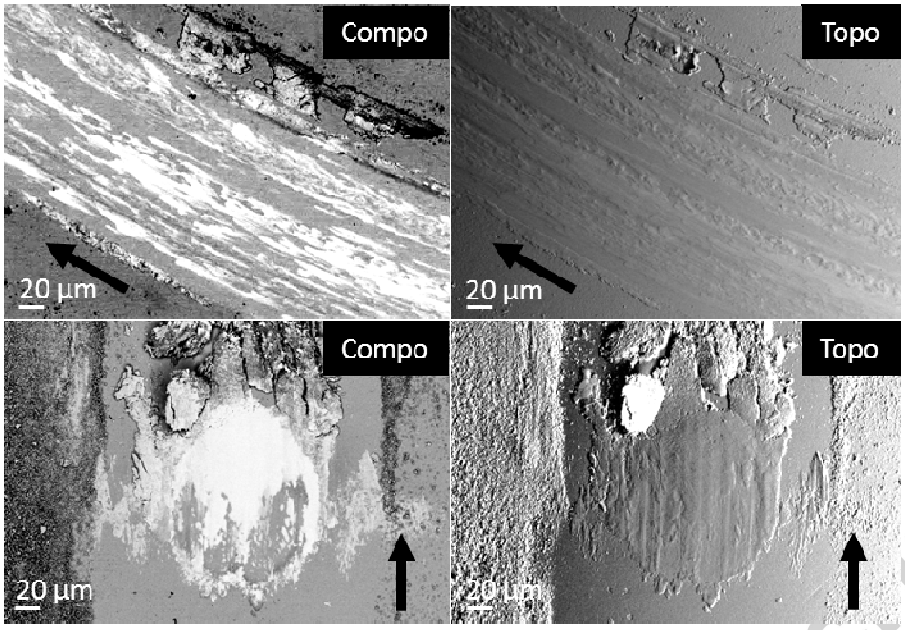

Figure 4: *Backscattered compositional (Compo) and topographical (Topo) images of the wear track (upper) and the corresponding transfer film on the steel balls (lower) for the MoSe-47C tested in dry air at 10 N. Sliding direction of the ball is indicated by an arrow in all images.*

EDX showed that the brighter areas were richer in selenium than the surroundings, while containing less carbon and oxygen. Molybdenum was evenly distributed in the wear track. However, higher concentration of molybdenum and oxygen was found along the sides of the wear track, see Fig. 5. The shape and topography of the wear scar on the ball indicated minimal wear of the ball. A large amount of coating material was adhered on the ball surface and, unlike the wear track on the coating, the transferred material appeared homogeneous with a chemical composition similar to the bright areas described above (i.e. rich in selenium).

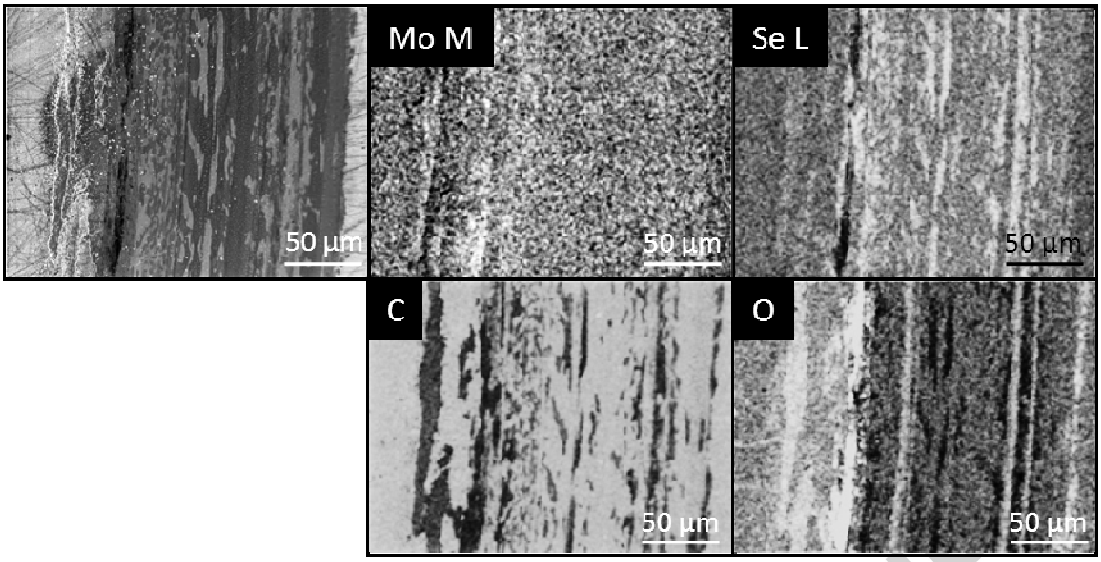

Figure 5: *SEM micrograph (left) and EDX elemental maps of the wear track for the MoSe-47C coating tested in dry air at 10 N load. The maps were acquired at 2 kV to increase surface sensitivity.*

Raman spectra of bright areas of the wear tracks showed only sharp peaks at the approximate wavenumbers 238 and 289 cm^{-1}, which were addressed to A^1_g and E^1_{2g} modes of $MoSe_2$ [22], see Fig. 6. Barely visible peaks positioned around 445 and 596 cm^{-1} together with the broad peak at 155 cm^{-1} are believed to be combination modes and second order Raman peaks for $MoSe_2$ [22], and similar features have been observed for MoS_2, which has the same electronic structure as $MoSe_2$ [23]. The broadening of the peak at ~289 cm^{-1} could in some cases be related to the presence of MoO_3 (approx. 285 cm^{-1}); however, much stronger MoO_3 modes at ~666, 850 and 995 cm^{-1} were not observed [23]. In fact, SeO_2 exhibit peaks at 290 and 594 cm^{-1}, which might overlap with $MoSe_2$. However, our previous TEM investigation of similar coatings or the TEM analysis shown below do not indicate any existence of SeO_2 [24]. It is believed that SeO_2 (if formed) leaves the contact in gas phase due to its very low sublimation temperature and the conditions occurring in the nanoscale contact of the asperities (high pressure and increased temperatures due to frictional heating) [24]. Also, the EDX maps did

not show any overlap between O and Se in the wear track. We can thus conclude that the bright area consists almost exclusively of $MoSe_2$. Furthermore, the sharp Raman peaks suggest that $MoSe_2$ is highly ordered. The Raman spectra taken from darker areas are similar to that of the as-deposited coating (Fig. 6), i.e. it shows D- and G-bands for carbon positioned around 1360-1370 cm^{-1} and 1580-1585 cm^{-1}, respectively, and broad and less pronounced peaks corresponding to $MoSe_2$. The carbon peaks suggests that the carbon has a disordered graphitic structure [25]. If we consider the ratio between the carbon and $MoSe_2$ peak areas as an indication of the chemical composition, then the darker areas in the wear track contained slightly more carbon than the as-deposited state. Finally, the material accumulated along the sides of the wear track consisted mostly of $MoSe_2$ with small amounts of carbon and molybdenum oxide.

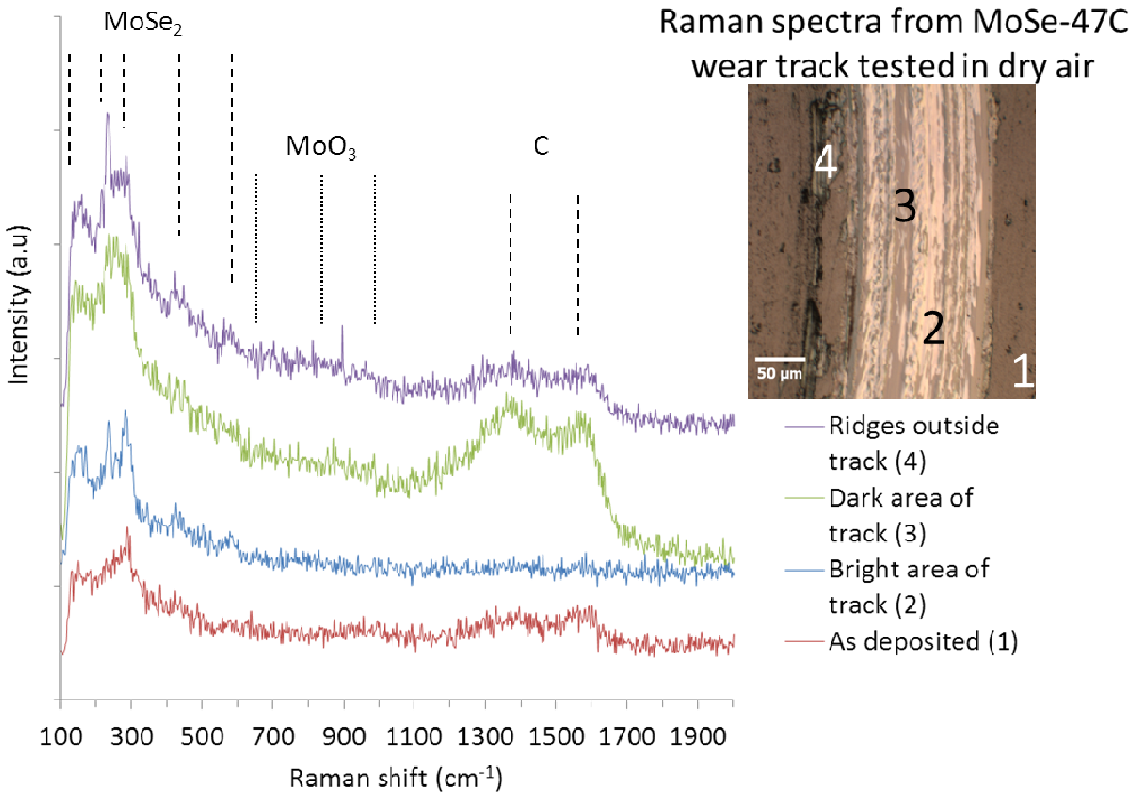

Figure 6: *Raman spectra acquired at different parts of the wear track for the MoSe-47C coating tested in dry air at 10 N load. Peak positions for $MoSe_2$, MoO_3 and carbon are indicated.*

3.4 Investigation of the worn surfaces – MoSe-61C

Optical images of the wear tracks and the ball surfaces from the tests with the MoSe-61C coating shown in Fig. 3 were similar to that of the MoSe-47C coating. However, we did not observe any delamination; the wear tracks were smoother and formation of bright areas described above less evident. In humid air, the friction was about 5 times higher than in Ar, which is still exceptionally low for an unlubricated contact in humid air. Moreover, the wear rate was at the same level or even slightly lower in humid air than in Ar. Thus, thorough analysis was performed for these two extremes to investigate the origin of the higher friction exhibited in humid air.

SEM/EDX analysis showed relatively thick and smooth layers containing mostly molybdenum and selenium. The highest content of carbon and oxygen was observed at the edges of the contact area and in the wear debris along its sides, see Fig. 7. Traces of iron at the rear of the transfer film indicate that the film is thinner there. The transfer films formed in Ar (not shown) and in humid air (Fig. 7) were very similar.

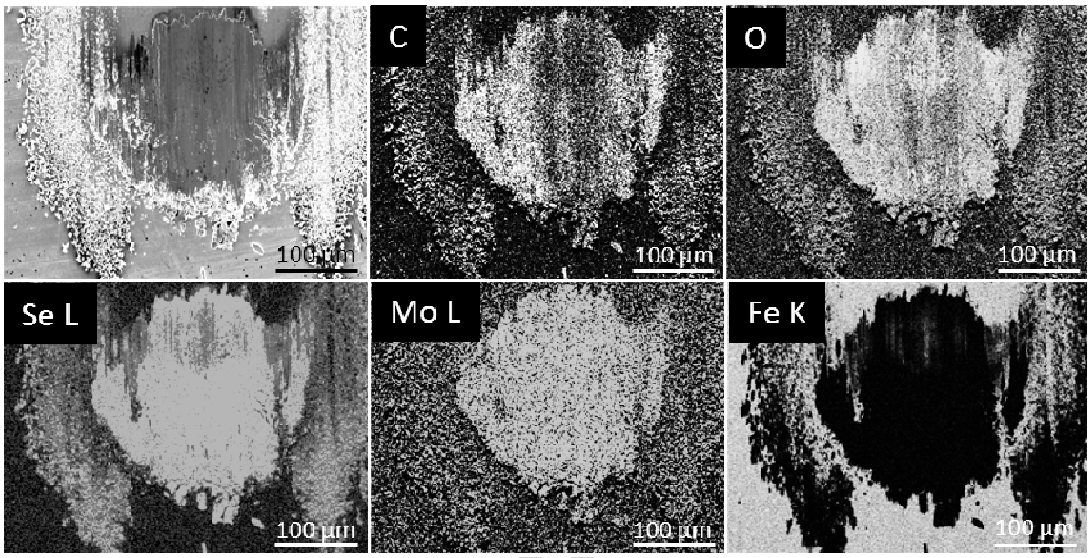

Figure 7: *SEM micrograph and EDX elemental maps of the transfer film on the steel ball run against MoSe-61C in humid air at 5 N load, acquired at 10 kV. The sliding direction of the counter surface is from bottom to top in the picture. The maps show only the distribution of each element in the contact and should not be interpreted quantitatively.*

XPS spectra of the films formed on the balls sliding against the MoSe-61C coating tested in humid air are shown in Fig. 8. If no other reference is given, Handbook of X-ray spectroscopy [26] was used for peak identification. The Mo $3d_{5/2}$ peak positioned at a binding energy of 228.2-228.4 eV in all three measurements matches well with $MoSe_2$ (228.3 eV). There is a very small peak positioned at 230 eV, which was identified as a $MoSe_xO_y$ compound [27]. No peaks corresponding to MoO_3 or MoO_2 were detected (235.5-236 eV), i.e. they were not necessary to achieve good fitting to the Mo $3d_{5/2}$ peak. Therefore, the amount of molybdenum

oxides should be negligible. The O 1s spectrum was deconvoluted into two peaks: i) a dominant peak positioned at 530.3-530.4 eV, which corresponds either to MoO_3 (530.4 eV) or Fe_2O_3 (530.2 eV), and ii) a small peak at ~532.1 eV again indicating the Mo-Se-O compound [27]. The dominant peak disappears by further etching, indicating it should mainly be present in the top surface region. Since hardly any contribution from MoO_2 or MoO_3 was observed in the Mo $3d_{5/2}$ spectrum, it is very probable that oxygen was bonded to iron. Overview spectra acquired with lower resolution (not shown here) displayed that Fe $2p_{3/2}$ had a slightly broadened peak at 710.3-710.4, which supports the presence of iron oxides [28]. Although SEM/EDX did not show iron in the transfer film, the indication of iron oxide in the XPS spectrum was not surprising. Probably the XPS signal originated not only from the transfer film, but also from the ball surface, since the analysis spot is wide and the precise alignment of the ball is very challenging. It should be noted that the oxygen signal was much weaker after longer surface etching, suggesting that the oxide was very superficial.

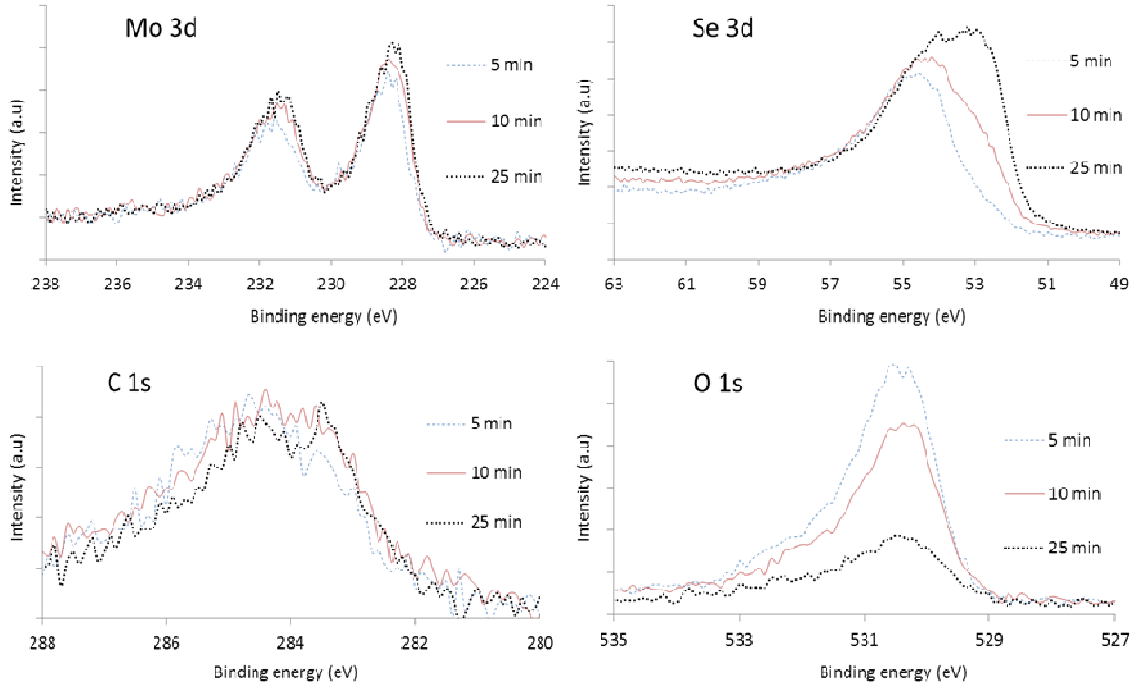

Figure 8: *XPS spectra from the transfer film formed on the steel ball run against the MoSe-61C coating at 5 N load in humid air. The spectra are normalized.*

The Se $3d_{5/2}$ spectrum changed significantly when the etching time was increased, see Fig.8. After 5 minutes etching, two peaks were identified. The first was positioned at a binding energy of 54.6-54.7 eV typical of $MoSe_2$ (54.6 eV), and the second at ~56 eV. The second peak matched well with Fe_2O_3 (Fe 3p peak) [28]. This presence of iron oxide corroborates the detection of the Fe 2p peak in the overview spectrum (not shown). After 15 and particularly after 25 minutes of sputter etching, a new peak appeared around 52.5 eV. This was associated with the 3p peak of iron originating from the ball surface [28]. The C 1s peak at 284.4-284.6 eV is typical for C-C bonds of amorphous carbon or graphite. After 25 minutes of sputtering, a small carbide contribution could be seen in the C 1s spectra; confirming that parts of the XPS signal originates from the ball surface outside the transfer film. The Fe $2p_{3/2}$ peak from the overview spectra (not shown) then was positioned at 707.2 eV, indicating mostly metallic iron. However, a small iron carbide contribution (~708.1 eV) is not unlikely, but would be difficult to deconvolute due to the poor resolution in the overview spectra.

XPS spectra of the transfer film on steel ball run against MoSeC-61C coating in Ar are presented in Fig. 9. Mo $3d_{5/2}$ and Se $3d_{5/2}$ indicate the presence of $MoSe_2$ and negligible amount of oxides. The same broadening of the Se 3d spectra appeared after 25 minutes of sputtering and the C 1s spectra show mainly C-C bonds, with only a small contribution of carbide. In fact, the transfer films produced in humid air and argon yielded almost identical XPS spectra.

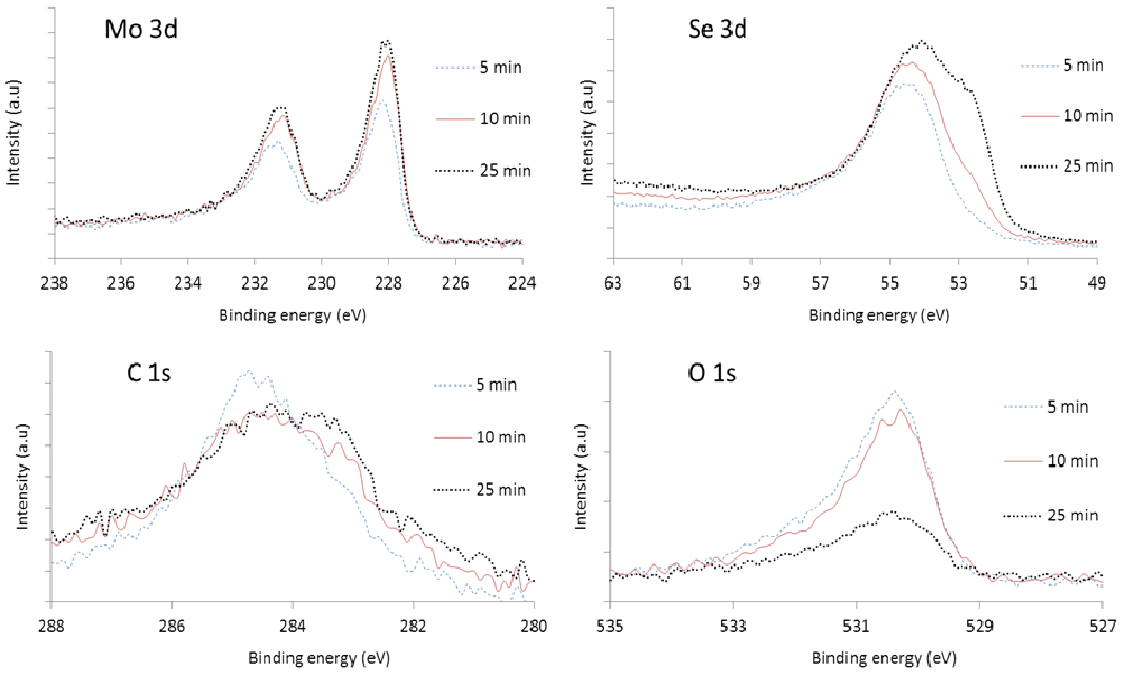

Figure 9: *XPS spectra from the transfer film formed on the steel ball run against the MoSe-61C coating at 5 N load in Ar atmosphere. The spectra are normalized.*

Raman analysis of the transfer films produced on the balls in humid air showed that the intensity ratio between $MoSe_2$ and C was highest in the center and decreased towards the edges of the wear scar. Also, the sharp $MoSe_2$ peaks in the center typical of highly ordered structures were much broader at the edges of the wear scar, indicating a less organized structure. It was expected, since the formation of well-ordered $MoSe_2$ structure is related to local contact pressure [14] and the pressure is the highest in the center of the wear track. The wear debris consisted mainly of disordered graphitic carbon and less-ordered $MoSe_2$. In some spectra, small peaks close to the regions corresponding to MoO_3 were observed. The center of the transfer film produced in argon showed almost exclusively $MoSe_2$ peaks; carbon was clearly moved from the center of the contact to the sides, see Fig. 10. This finding corroborates our previous studies on similar self-lubricant systems [3,14]. The presence of

carbon peaks in the center of the wear track produced in humid air might indicate thinner $MoSe_2$ tribolayer compared to that formed in argon.

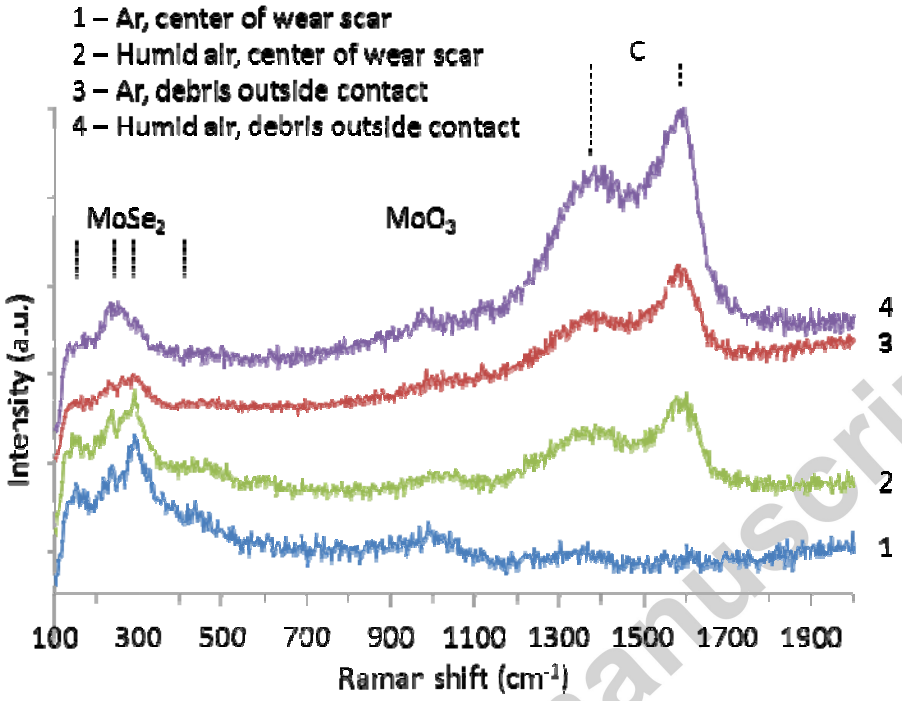

Figure 10: *Raman spectra from the transfer films on the steel balls run against MoSe-61C in Ar and humid air at 10 N load. Spectra were acquired from the center of the contact and from the debris accumulated along the sides of the contact.*

Four TEM cross sections were prepared using FIB; one from the center of the wear track on the MoSe-61C coating and one from the center of the transfer film on the corresponding ball, from the 10 N load tests in humid air and in Ar.

To assure that the TEM samples from the wear tracks included the zone of the highest pressure, the cross sections were cut perpendicular to the sliding direction. The TEM cross sections of the transfer films on the balls were cut parallel to the sliding direction.

In the wear track formed in humid air, a clear structural change had occurred in the top 20 nm. Here, a structured tribofilm with basal planes aligned parallel to the sliding surface had

formed, see Fig. 11. The interplanar distances, 6.4-6.5 Å, correspond to $MoSe_2$ [1]. Below this tribofilm, small, thin randomly oriented layers of $MoSe_2$ were embedded in a carbon matrix, resembling the as-deposited coating. EFTEM elemental maps of the tribofilm verified that it was predominantly formed by $MoSe_2$ and almost free from carbon, see Fig. 11.

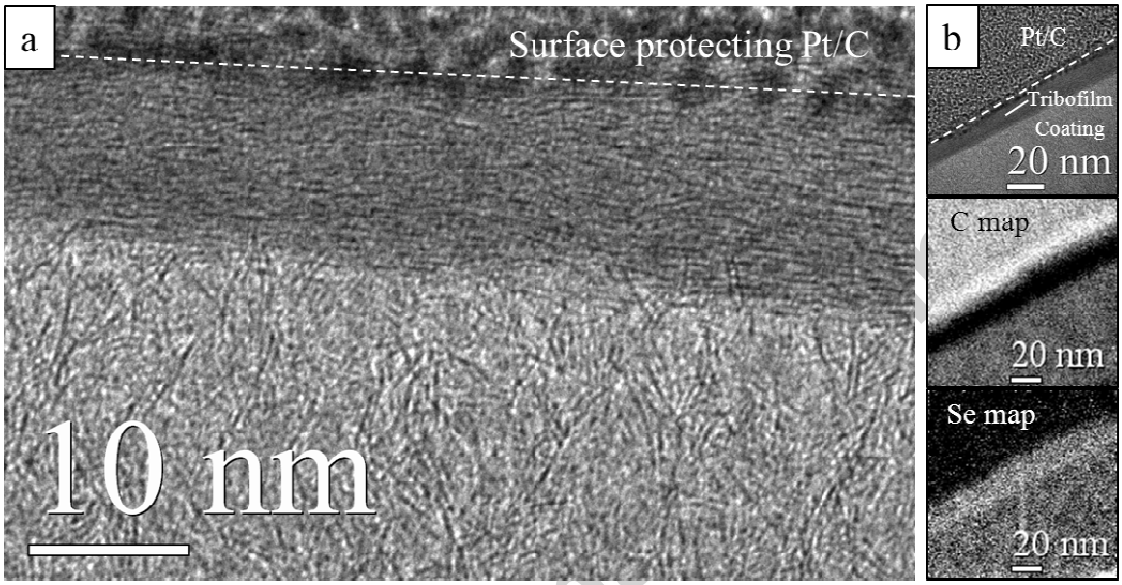

Figure 11: a) *TEM cut perpendicular to the sliding direction from the wear track of the MoSe-61C coating tested in humid air at 10 N load. A clear structural change involving formation and alignment of $MoSe_2$ planes parallel to the sliding surface has taken place down to a depth of 20 nm. b) TEM of the same area and EFTEM maps of the film showing a depletion of carbon and an enrichment of Se in the structurally changed area.*

The transfer film on the ball was approximately 400 nm thick consisting mostly of crystalline $MoSe_2$. The top part of the transfer film is shown in Fig. 12. Although the basal planes again were mostly oriented along the sliding direction, the degree of alignment was lower than on the coating side.

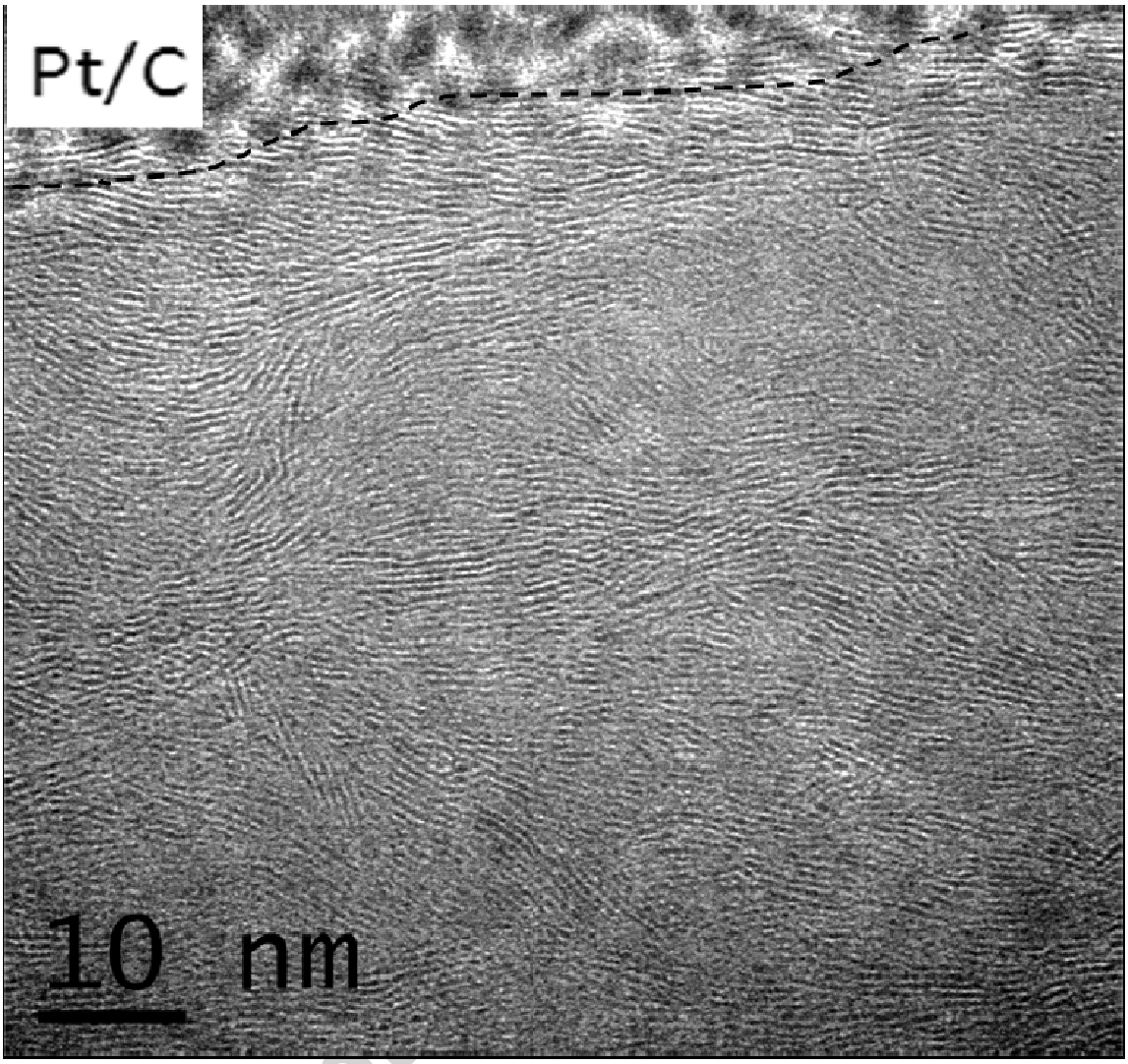

Figure 12: *TEM image of the transfer film formed on the steel ball run against the MoSe-61C coating at 10 N load in humid air.*

In the STEM, the strong atomic number contrast revealed particles or agglomerates with sizes up to a few hundred nanometers. The darker contrast indicated that the mean atomic number is lower than that of the surrounding $MoSe_2$. STEM EDX mapping confirmed that the transfer film mainly consists of Mo and Se with only small amounts of carbon, and proved that the particles/agglomerates contained exclusively oxygen and molybdenum, see Fig. 13. Iron was

not detected in the transfer film. STEM-EELS SI validated the STEM EDX-data; the fine structure of the oxygen K edge in the EELS spectra from the larger agglomerates matched with MoO_3 reference spectra (not shown).

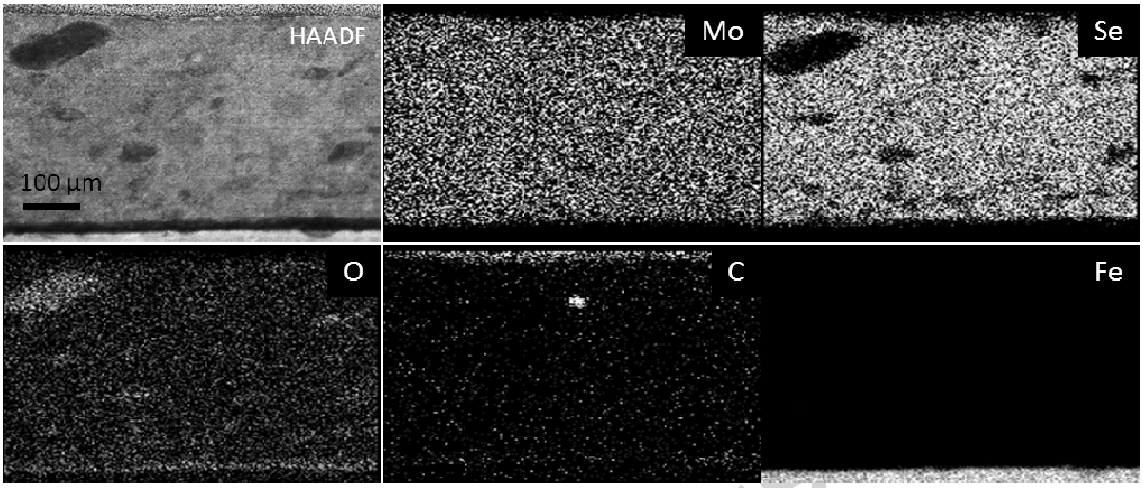

Figure 13: *STEM HAADF image and XEDS maps of the transfer film. The darker areas in the HAADF image only give signal from Mo and O.*

Also, the tribofilm formed in the wear track produced when sliding in Ar was topped by a very thin, well-ordered $MoSe_2$ (again with the basal planes parallel to the sliding surface), see Fig. 14a. The corresponding film transferred to the steel ball showed a thickness similar to that formed in humid air (150-300 nm) and consisted almost exclusively of highly crystalline $MoSe_2$ with the basal planes aligned parallel to the surface (Fig. 14b).

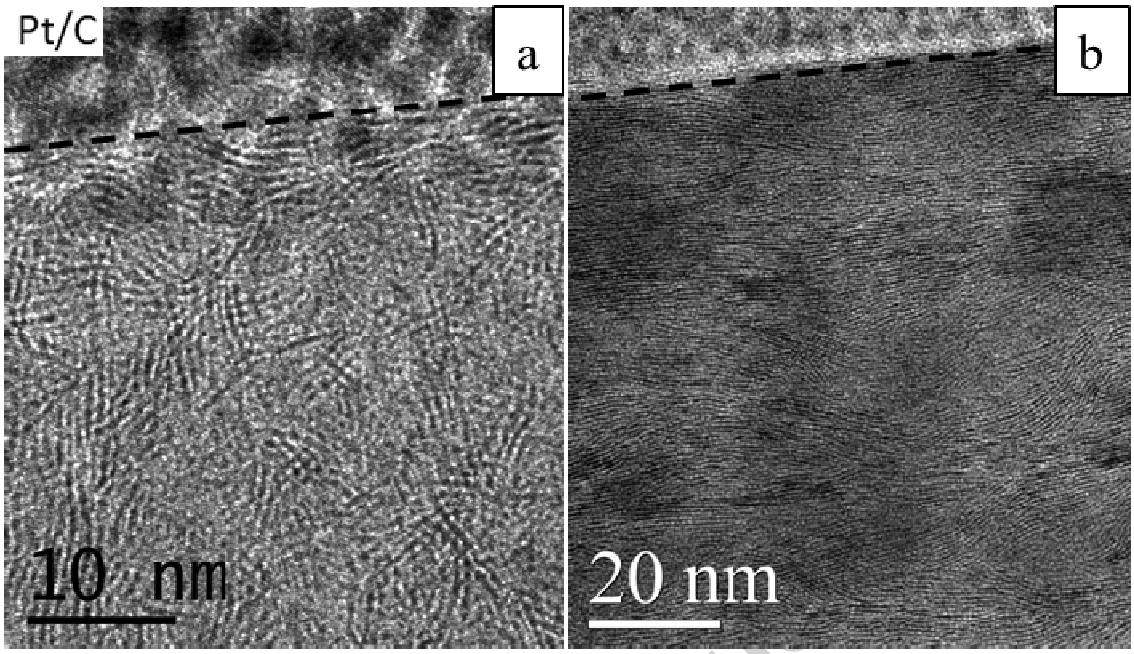

Figure 14: *a) HR TEM of the wear track formed on the MoSe-61C coating tested at 10 N load in Ar. The FIB cut was prepared perpendicular to the sliding. b) HR TEM image of the corresponding transfer film on the steel ball; the FIB cut parallel to the sliding.*

4. Discussion

4.1 Tribological and analytical results

The friction of the investigated coatings was lower at higher loads, which is typical for TMDs (pure as well as doped or alloyed with other elements). The friction coefficient was similar in argon, nitrogen and dry air but significantly higher in humid air. Both coatings exhibited remarkably low wear rates (except for local adhesive failures of the MoSe-47C coating) corresponding to approximately one molecular layer per 10-20 passages of the ball (cycles). Moreover, the wear rate during the steady state sliding should be significantly lower, since the transfer of the coating material to the ball during the running-in process represents a

significant amount of the volume worn from the coating [14]. The wear tracks formed in dry air and, to some extent, in nitrogen and humid air exhibited two pronounced variations in the composition: (i) streaks consisting of almost pure $MoSe_2$, smeared along the sliding direction, and (ii) the remaining area, with an appearance similar the as-deposited coating. Interestingly, the areas rich in $MoSe_2$ were typically located higher in the wear track, while the lower parts have probably been in less contact, since the composition and structure, as identified with Raman, are similar to that of the as-deposited coating.

4.2. Wear mechanisms

Based on the compositional variation and structure found on the worn surfaces, we suggest that coating material is first removed from the coating, then adhered on the ball surface where the carbon is separated from the $MoSe_2$ and transported towards the side of the wear scar (which is supported by the gradient in carbon shown in Fig. 7), and finally the $MoSe_2$ enriched material becomes transferred back to the coating surface. We did not observe any carbon at the sliding interface and it seems that carbon does not play any significant role in the sliding. It corroborates our previous studies on similar W-S-C and Mo-Se-C systems [5,14,29], where the carbon was not found on the top surface of the wear tracks. The very low friction coefficients in argon and nitrogen support our hypothesis, since hydrogen-free amorphous carbon films are known for high friction in these environments [30,31].

4.3 Effect of humidity

The oxidation of the TMD-based materials is often considered as the main reason for high friction in humid air [32,33]. Martin et al. [34] showed that pure MoS_2 could be considered as a “superlubricant” in ultra-high vacuum conditions (the friction was below the resolution of the equipment). They observed that the friction became higher when the partial pressure of

oxygen in the vacuum chamber was increased. The effect on friction of oxygen atoms replacing sulfur in MoS_2 crystals (i.e. $MoS_{2-x}O_x$) was studied by molecular dynamics in Ref. [35]. There the friction was the lowest for pure MoS_2 and then increased with x. It reached a maximum at x = 0.25 and then decreased again. The authors suggested that the increase of the friction was due to a reduction of the interlayer Coulomb repulsion and a surface roughening at the atomic scale due to the replacement of sulfur atoms by oxygen. When the number of oxygen atoms was higher, the surface was smoothened again and, consequently, the friction decreased. This simulation supported older results presented by Fleischauer and Lince [36], who highlighted the difference between oxidation (i.e. formation of MoO_3) and oxygen substitution ($MoS_{2-x}O_x$). The former was always detrimental, leading to high friction and accelerated wear, whereas the latter did not substantially degrade the tribological performance. They pointed out that the substitution was typical of as-deposited sputtered films (oxygen from the residual atmosphere) and oxidation was the process occurring during storage, particularly in humid air, or during the sliding process in oxygen-containing atmospheres. Our results (XPS, TEM, and Raman spectroscopy) showed a very low level of oxygen both in the tribofilm formed in the wear track and in the transfer film on the ball after the tests in humid air. In fact, there was almost no difference in the oxygen content between the tests in argon and in humid air. Moreover, Raman showed very low amounts of oxides, and XPS analyses suggested that the only oxygen present in the transfer film was in the form of $MoSe_{2-x}O_x$. Considering the analogy between MoS_2 and $MoSe_2$, we could expect that the friction should still be very low even though oxygen atoms were introduced in the $MoSe_2$ structure [35].

However, the agglomerates found in the transfer film formed on the ball in humid air were proven by EELS to be MoO_3, the most stable oxide for Mo. These agglomerates should not influence the friction to any larger extent since they were never found close to the sliding

interface. Considering wear, MoO_3 particles are known to be capable of causing abrasive wear of the formed tribofilms [37,38]; however, the wear rate in this work was almost identical when sliding in argon and humid air. Since molybdenum oxide particles were not observed in the transfer film formed in argon atmosphere, it is therefore probable that these agglomerates were during the sliding in humid air either removed from the contact by the same mechanism as described above for carbon, or they remained embedded in the transfer film. Thus, high friction in humid air cannot be fully explained by oxidation of the $MoSe_2$. The comparison of TEM cross-sections (Fig. 11 and Fig. 14) suggests that the well-aligned $MoSe_2$ tribofilm was thicker in the wear track produced in humid air (approx. 20 nm) than in argon (approx. 5 nm, i.e. few molecular layers). However, these thicknesses observed in TEM are not necessarily representative for the entire sliding process. The sliding interface may very well shift between different possible easy shear planes. Such shifts may take place locally and perhaps be very frequent. They can be caused by the local roughness of the surfaces (the roughness is large in comparison to the tribofilm thickness) or other factors disturbing the shear stress distribution or the local shear strength of the film. Up or down shift of the sliding interface will of course be coupled to transfer of layers to the ball or the coating. We believe that the adhesive mechanism of this type frequently and locally alters the thickness of the tribofilm on the two sides of the contact. In our previous study we observed different thicknesses of the tribofilm in different spots in one wear track (Mo-Se-C coating with 51 at.% of carbon [29]). Regardless of its thickness, we conclude that the material composition at the sliding interface is identical, almost exclusive $MoSe_2$, and that its crystallographic orientation is optimal to achieve the lowest friction [39]. Based upon the results discussed above we can propose that the detrimental effect of the water molecules is primarily due to their adsorption in the $MoSe_2$ sliding interface, where they temporarily increase the interfacial shear strength [38]. Higher load could then compress the structure further, making it more difficult for the water

molecules to enter between the layers, and as a result decrease the friction coefficient. The reason for higher wear in dry air and in N_2 has not been investigated and therefore remains unsolved. Due to the excellent tribological performance in argon, humidity is not believed to be the important factor here.

4.4 The role of carbon

Why did the MoSe-61C coating, with higher carbon content, show lower friction coefficients than the MoSe-47C coating? For this family of coatings, carbon has proven to increase the hardness, and correspondingly the shear strength increases, which could be expected to increase the friction. The answer lies in that after the tribological contact, the much softer, pure $MoSe_2$ totally dominates the sliding interface for both carbon contents. In this way, the more ideal friction situation is achieved for the harder coating. The higher hardness leads to a smaller contact area to shear, and interfacial shear strength is the same, since the interfacial layer is transformed to the same, very easily sheared $MoSe_2$. This transformation is rather remarkable: it includes the preferential elimination of carbon from the structure, aggradation of the small $MoSe_2$ structures into larger crystals, and finally an efficient orientation of these crystals into the ideal angle with the easy shear planes parallel to the sliding direction, i.e. basal plane-on-basal plane interfacial sliding. An interesting question is now how the carbon is so efficiently depleted? In the present case 47 and 61 at.% carbon, respectively, has been virtually eliminated. Does this mechanism operate on the atomic level by diffusion mechanisms, or on a larger scale?

In humid air, the presence of graphite in MoS_2 based coatings has been suggested to work as an oxygen getter. The carbon is more prone to oxidize, thereby it collects the oxygen in the structure and consequently reduces the negative effect on the MoS_2 [15]. If an equivalent effect holds also for $MoSe_2$, then carbon could be suggested to be removed in gaseous form

by oxidation. However, when sliding in argon, hardly any oxygen is present and still the carbon is efficiently removed from the contact. This indicates that removal in gaseous form is not a very likely mechanism.

The fact that carbon rich layers and debris are found around the periphery of the wear scar on the ball and along the wear track on the coating indicates that there could be some mechanism based on "preferential removal" of carbon rich wear debris. The carbon rich debris is distributed much like it would have been by a snow plough, indicating that it is first pushed in front of the ball and then gradually moved to the sides until it eventually falls outside the plough, resting either on the coating side or on the ball. One possible mechanism behind this preferential removal would be if more carbon rich debris has a stronger tendency to be ploughed away rather than enter into the narrow gap between the ball and the flat. This tendency would be stronger for larger particles and less easily sheared particles (i.e. those more resistant to become squeezed between the surfaces). Carbon rich particles should be expected to be harder, and therefore less easily sheared. Since microscopic wear particles are continuously created, and then repeatedly "sorted" at each passage of the ball, the suggested mechanism could lead to a gradual removal of more carbon rich material, corresponding to a gradual enrichment of Mo and Se in the contact area. With less surrounding carbon the original microscopic $MoSe_2$ platelets have a better possibility to sinter and form much more extensive planes, eventually leading to the well aligned structures revealed in the TEM.

There is significant experimental evidence that such separation is typical for various nanostructured systems combining TMD and other phases. Scharf et al. has shown formation of exclusive MoS_2 tribolayer in case of sliding of MoS_2/Sb_2O_3/Au nanocomposite coating [40]; MoS_2 was well-ordered with basal planes parallel to the surface after sliding in nitrogen and humid air. Nyberg et al. has recently published a study on tribological behaviour of W-S-C-Ti coatings, where WS_2 tribolayer was formed during sliding in dry air [41]. The results of

Fominski et al. suggest that TMD tribolayer is formed in case of W-Se-C [42] and Mo-Se-Ni-C [43] coatings. Our previous studies on TMD-C coatings [29] and complex analysis of amorphous W-S-C-Cr films [3] has indicated the formation of a TMD low-friction tribolayer as well. In fact, the first observation of well-aligned MoS_2 layers in the contact was observed by Wahl et al. in their pioneering work on amorphous Mo-Pb-S system [44].

The exact mechanisms and driving forces for the separation and/or formation of TMD tribolayer is obviously not clear, and should be further investigated by dedicated experiments and simulations.

Conclusions

Two Mo-Se-C coatings deposited by magnetron sputtering (containing 47% and 61% carbon, respectively) were tribologically evaluated against steel balls in different dry and humid atmospheres. Very low friction coefficients were found in several cases. The low-friction behavior was attributed to the formation and structural alignment of pure $MoSe_2$ layers in the sliding contact. Lower friction coefficients were achieved for the coating with higher C content. The wear rate was very low for both coatings, independently of the testing conditions and the carbon content. Although the friction in argon was 5 times lower than in humid air, the wear rate was almost identically low. Extensive analysis of worn surfaces did not indicate any correlation between the friction coefficient and the wear rate. During sliding, interfaces were depleted in carbon, and the relatively unordered structure became much more crystalline, resulting in only well-aligned $MoSe_2$ present in the interface, with its easy shear basal planes oriented along the sliding direction (basal plane-on-basal plane interfacial sliding). Oxygen was not observed in the contact area, and it was suggested that the humidity only affects the structure by increasing the shear strength, not by oxidizing the $MoSe_2$ to any significant extent. The results clearly demonstrate the promise of Mo-Se-C based coatings for

unlubricated tribological components used in ordinary humid air. The presently investigated coatings show a clear advantage over most coatings based on Mo and W sulfide, which give high friction and rapidly deteriorate in humid air.

Acknowledgements

This work was supported by the Czech Science Foundation through the project 108/10/0218. The support from the Swedish Research Council grant no. 2009-15941-70482-35 and from the Swedish Foundation for Strategic Research via the program Technical advancement through controlled tribofilms is gratefully acknowledged. Part of the experimental work was carried out at *the Canadian Centre for Electron Microscopy (CCEM)*, a national facility supported by *NSERC* and *McMaster University*. Funding from FEDER / COMPETE and FCT through project no. PTDC/CTM-MET/120550/2010 is also greatly acknowledged.

References

[1] Jamison WE, Cosgrove SL. A S L E Transactions 1971;14:62.

[2] Scharf TW, Rajendran a., Banerjee R, Sequeda F. Thin Solid Films 2009;517:5666.

[3] Polcar T, Gustavsson F, Thersleff T, Jacobson S, Cavaleiro A. Faraday Discussions 2012;156:383.

[4] Zabinski JS, Donley MS, Walck SD, Schneider TR, Mcdevitt NT. Tribology Transactions 1995;38:894.

[5] Polcar T, Evaristo M, Cavaleiro A. Plasma Processes and Polymers 2009;6:417.

[6] Voevodin AA, Fitz T a., Hu JJ, Zabinski JS. Journal of Vacuum Science & Technology A: Vacuum, Surfaces, and Films 2002;20:1434.

[7] Teer DG, Hampshire J, Fox V, Bellido-Gonzalez V. Surface and Coatings Technology 1997;94-95:572.

[8] Johnson RL, Sliney HE. Fundamental Considerations for Future Solid Lubricants. 1969.

[9] Kubart T, Polcar T, Kopecký L, Novák R, Nováková D. Surface and Coatings Technology 2005;193:230.

[10] Lavik MT, Medved TM, Moore GD. A S L E Transactions 1968;11:44.

[11] Brainard WA. The Thermal Stability and Friction of the Disulfides, Diselenides, and Ditellurides of Molybdenum and Tungsten in Vaccum (10 -9 to 10 -6 Torr). NASA technical report,1969 (http://ntrs.nasa.gov/archive/nasa/casi.ntrs.nasa.gov/19690013627_1969013627.pdf)

[12] Polcar T, Evaristo M, Cavaleiro A. Wear 2009;266:388.

[13] Evaristo M, Polcar T, Cavaleiro A. Vacuum 2009;83:1262.

[14] Polcar T, Evaristo M, Colaço R, Silviu Sandu C, Cavaleiro A. Acta Materialia 2008;56:5101.

[15] Gardos MN. Tribology Transactions 1988;31:214.

[16] Polcar T, Evaristo M, Stueber M, Cavaleiro a. Surface and Coatings Technology 2008;202:2418.

[17] Oliver WC, Pharr GM. Journal of Materials Research 2011;7:1564.

[18] Mcintyre NS, Spevack PA, Scrence S, Briggs D. 1990;237.

[19] Bernède J. Applied Surface Science 2001;171:15.

[20] Fusaro RL. A S L E Transactions 1982;25:141.

[21] Singer IL. Surface and Coatings Technology 1991;49:474.

[22] Sekine T, Izumi M, Nakashizu T, Uchinokura K, Matsuura E. Journal of the Physics Society Japan 1980;49:1069.

[23] Windom BC, Sawyer WG, Hahn DW. Tribology Letters 2011;42:301.

[24] Moore GD. A S L E Transactions 1970;13:117.

[25] Ferrari A, Robertson J. Physical Review B 2000;61:14095.

[26] J. F. Moulder, W. F. Stickle, P. E. Sobol KDB. Handbook of X-ray Photoelectron Spectroscopy. Physical Electronics, Inc.; 1995.

[27] Dukstiene N, Tatariskinaite L, Andrulevicius M. Materials Science-Poland 2010;28:93.

[28] Yamashita T, Hayes P. Applied Surface Science 2008;254:2441.

[29] Polcar T, Cavaleiro A. Surface and Coatings Technology 2011;206:686.

[30] Ronkainen H, Holmberg K. Environmental and Thermal Effects on the Tribological Performance of DLC Coatings, in: Donnet C, Erdemir A (Eds.). Tribology of Diamond-Like Carbon Films. Springer; 2008.

[31] Andersson J, Erck RA, Erdemir A. Wear 2003;254:1070.

[32] Lansdown AR. Molybdenum Disulphide Lubrication. Elsevier; 1999.

[33] Suzuki M. Lubrication engineering 2000;57:23.

[34] Martin J, Donnet C, Le Mogne T, Epicier T. Physical Review B 1993;48:10583.

[35] Onodera T, Morita Y, Nagumo R, Miura R, Suzuki A, Tsuboi H, Hatakeyama N, Endou A, Takaba H, Dassenoy F, Minfray C, Joly-Pottuz L, Kubo M, Martin J-M, Miyamoto A. Journal of Physical Chemistry B 2010;114:15832.

[36] Fleischauer PD, Lince JR. Tribology International 1999;32:627.

[37] Hirvonen J-P, Koskinen J, Jervis JR, Nastasi M. Surface and Coatings Technology 1996;80:139.

[38] Donnet C, Martin JM, Le Mogne T, Belin M. Tribology International 1996;29:123.

[39] Martin JM, Pascal H, Donnet C, Le Mogne T, Loubet JL, Epicier T. Surface and Coatings Technology 1994;68-69:427.

[40] Scharf, TW, Kotula, PG, Prasad, S.V. Acta Materialia 2010;58:4100

[41] Nyberg H et al., Extreme friction reductions during initial running-in of W–S–C–Ti low-friction coatings. Wear (2013), http://dx.doi.org/10.1016/j.wear.2013.01.065i

[42] Fominski, VYu, Grigoriev SN, Celis JP, Romanov RI, Oshurko VB. Thin Solid Films 2012; 520:6476

[43] Fominski, VYu, Grigoriev SN, Gnedovets AG, Romanov RI. Surface and Coatings Technology 2012; 206:5046

[44] Wahl KJ, Dunn DN, Singer IL. Wear 1999; 230:175

Highlights

- MoSeC coatings exhibited very low friction coefficient in different atmospheres.
- The wear rate was almost identical in dry nitrogen and humid air.
- $MoSe_2$ tribolayer observed after testing both in argon and humid air.
- The carbon is preferentially removed from the contact area.
- The presence of water vapour does not increase the surface oxidation.